Acta Crystallographica Section A
**Foundations of Crystallography**
ISSN 0108-7673

Received 20 March 2006
Accepted 14 December 2006

# Are intramolecular dynamic electron correlation effects detectable in X-ray diffraction experiments on molecular crystals?

**Ian Bytheway, Graham Chandler,* Brian Figgis and Dylan Jayatilaka**

Chemistry, School of Biomedical and Chemical Sciences, The University of Western Australia, Crawley 6009, Australia. Correspondence e-mail: gsc@chem.uwa.edu.au

In order to assess whether the effects of intramolecular dynamic electron correlation on the electron density would be experimentally detectable, X-ray structure factors which include thermal averaging effects have been calculated from the electron densities of a range of small-molecule molecular crystals [$C_2H_6$, $C_2H_4$, $C_2H_2$, $BH_3NH_3$, $NH_3$, $NH_2CN$, $OCl_2$, $CO(NH_2)_2$] using the procrystal, Hartree–Fock, B3LYP and QCISD wavefunction models with the superposition-of-independent-molecules method to create the electron density in the crystal. A naive *R*-factor-like criterion of 1% has been used to assess detectability, as well as a more sophisticated method based on real X-ray data for estimating experimental errors. Correlation effects on the density are found to be only marginally above the 1% detectability threshold, and are about one to two orders of magnitude smaller than deviations from the procrystal model. Further, only 10% of the data up to 1.2 $\text{Å}^{-1}$ are significant for detecting correlation effects; and of those 10%, many are at low intensity and therefore difficult to measure. Another method to estimate the experimental errors indicates that the intramolecular correlation effects would not be measurable. Although thermal averaging effects are important for the absolute value of the calculated structure factors, the use of different thermal averaging models does not change our overall conclusion of detectability. Likewise, calculations using the B3LYP method for some molecules do not show significant changes in the amount of, or distribution of, the changes that would be detectable by experiment.



## 1. Introduction

The topic of electron correlation in chemistry is of paramount importance. Electron correlation is a generic term that refers to effects related to the instantaneous (as opposed to the average) distribution of the electrons in a molecule or in a solid, and it contributes significantly to many physical and chemical properties; for example, to chemical reaction energies. Although the effect of electron correlation on any property is easily defined (as the difference between the exact value and the value of the property calculated using the mean-field or Hartree–Fock approximation), it is difficult to model correctly. What is commonly spoken of as correlation is dynamic correlation, where it is assumed that the Hartree–Fock determinant is a good first approximation. Correlation is then correcting for the inadequacies of the Hartree–Fock Hamiltonian, which contains the average electronic potential instead of the instantaneous potential. When there are near degeneracies, the Hartree–Fock determinant is no longer a good approximation, and other configurations mix in strongly, leading to much larger correlation effects, generally called non-dynamical effects (Sinanoğlu, 1961; Silverstone & Sinanoğlu, 1966; Hollister & Sinanoğlu, 1966). The molecules chosen for this study do not display these non-dynamical effects. Despite the problems of electron correlation, near exact properties can be obtained for small molecules, typically using wavefunction calculations that can be systematically improved by extrapolation of various parameters, albeit with great computational effort [see, for example, Helgaker *et al.* (2000)]. Recently, however, there has been much progress in density functional theory (DFT), which, although not systematically improvable, can nevertheless produce accurate results at much reduced computational expense [see, for example, Chong (1995) or Chong (1997)]. DFT is concerned with the calculation of properties of molecular and crystalline quantum systems using only the electron density as the prime variable to calculate (among other properties) the correlation energy, *i.e.*, in DFT, the wavefunction is eliminated as the unknown quantity in favour of the electron density.

In relation to electron correlation, the interest in density functional theory, and the electron density on which it is based, prompts two obvious questions:

1. How large are the changes in the electron density due to electron correlation, these changes which contribute so significantly to the physical and chemical properties of a system?

2. Are these changes in the electron density experimentally detectable?

Concerning the first question, there is quite a body of literature concerning the analysis of electron correlation effects on the electron density in real space, either by comparing difference density maps (Bader & Chandra, 1968; Smith, 1977; Coppens & Hall, 1982; Stephens & Becker, 1983; Ritchie *et al.*, 1986; Moszynski & Szalewicz, 1987), or by using topological properties of the total electron density in real space (Gatti *et al.*, 1988), or by using both (Boyd & Wang, 1989). There have also been studies of the effects of electron correlation on the electron density in real space using wave-function-based methods such MP2 and QCISD, as well as DFT-based methods (Boyd & Wang, 1989; Wang, Eriksson *et al.*, 1994; Wang, Shi *et al.*, 1994; Wang, Eriksson *et al.*, 1996; Wang, Johnson *et al.*, 1996; Boyd *et al.*, 1995; Ortiz-Henarejos & San-Fabian, 1997).

The comparison of static electron-density maps (*i.e.* maps that do not account for the effect of thermal vibration of the nuclei) for studying the changes due to electron correlation, although legitimate when comparing two different theoretical methods, is problematic if one wishes to address the question of whether such changes are experimentally detectable. The problem is that it is difficult to estimate the experimental errors in these static electron-density maps. To obtain the static maps, a model must be used to fit the observed structure-factor data [see, for example, Coppens (1997); Howard *et al.* (1992); Jayatilaka & Grimwood (2001)] and the static electron-density maps contain errors due to assumptions in these models. (These model-dependent errors can never be eliminated, even in principle, because the concept of a static electron density itself is only meaningful within the Born–Oppenheimer model.) Furthermore, even though it is possible to make a map of the errors in the static electron-density plots arising from uncertainties in the experimental measurements for a particular crystal (Coppens, 1997), it is difficult to predict what such errors will be in general, because the electron density at any point includes contributions from many structure factors.

In contrast to work on static electron-density maps, there has been relatively little work concerning the size of electron correlation effects on the structure factors of the electron density. Recently, though, collaborators with Feil (Zavodnik *et al.*, 1999; van Reeuwijk *et al.*, 2000) have used X-ray structure factors in their comparisons between experimental and theoretical results for urea, $NH_4F$ and $NH_4HF_2$. In the course of their study (which was more concerned with the interaction density than with electron correlation), they reported the difference in structure factors obtained from Hartree–Fock and density functional calculations. The findings were reported as partial $R$ factors over ranges of $\sin\theta/\lambda$ expressing the difference between the structure factors calculated by the various quantum-mechanical methods.

In view of the problems with static electron-density maps, the best way to address the question of the size of the electron correlation effects is to compare the X-ray structure factors – the quantities most closely related to the experimental measurement. We display the distribution of the effect of electron correlation on the structure factors at different scattering angles and as a function of the intensity of a particular X-ray reflection, and we discuss how many of these reflections show a significant change, *i.e.* we give an indication of how much of the X-ray diffraction data is significant from the point of view of electron correlation. Another way to address the question of the size of the correlation effects on the electron density is to offer a comparison relative to some other effect. Therefore, we also present in this paper an analysis of the effects of chemical bonding, *i.e.* the deviations of the electron-density structure factors from the promolecule or superposition of atoms model. We make this basic comparison not only to highlight the effects of correlation relative to chemical bonding effects but for the added insights it may give to the determination of chemical bonding effects from X-ray data. Earlier work (Dawson, 1967; Stewart, 1976; Bentley & Stewart, 1976; Epstein *et al.*, 1977; Coppens, 1997) stimulated a considerable amount of investigation that has been directed to using X-ray data to obtain difference density maps that show the re-organization of electrons that occur on molecule formation. However, since it was not necessary in those studies, their work did not specifically address the question of the size of these chemical bonding effects. Nevertheless, Zavodnik *et al.* (1999) have addressed this matter by comparing partial $R$ factors for spherical-atom and multipole refinements that showed differences of up to 3% at low scattering angles. We present more detailed information for a range of molecules here.

The second question of whether the changes in the structure factors due to electron correlation are experimentally detectable is addressed in the next section. In this paper, we restrict our attention to the X-ray diffraction experiment and, in particular, to molecular crystals of small-molecule compounds. The X-ray diffraction experiment has been chosen because it is widely used to study the electron density; the intensities of X-ray crystal diffraction spots are related to the Fourier transform of the thermally averaged electron density – the so-called structure factors. We have chosen small-molecule molecular compounds since these are the most amenable to theoretical calculation. Other experimental techniques such as Compton scattering or electron diffraction, or combinations of these techniques with X-ray diffraction (Becker *et al.*, 2001; Streltsov *et al.*, 2003), may be argued to be more sensitive for studying the effects of electron correlation, but these are not considered further here. Nevertheless, since electron diffraction can also yield electron-density structure factors, the results of an answer to this second question may be relevant to that experiment.

**Table 1**
The number of structure factors $N_{>1\%}$ which have $R_{\rm HF:QCISD} > 0.01$, and the number of structure factors $N_{\rm IAM>1\%}$ that have $R_{\rm IAM:QCISD} > 0.01$ compared to the total number of structure factors $N$ with $\sin\theta/\lambda \leq 1.2$ Å$^{-1}$ for a selection of small-molecule molecular crystals.

| Molecule | $N_{\rm IAM>1\%}$ | $N_{>1\%}$ | $N$ | $N_{\rm IAM>1\%}/N$ | $N_{>1\%}/N$ | Reference |
|---|---|---|---|---|---|---|
| $C_2H_6$ | 725 | 104 | 1033 | 0.70 | 0.10 | van Nes & Vos (1978) |
| $C_2H_4$ | 465 | 88 | 869 | 0.53 | 0.10 | van Nes & Vos (1979) |
| $C_2H_2$ | 207 | 77 | 387 | 0.53 | 0.20 | McMullan *et al.* (1992) |
| $BH_3NH_3$ | 863 | 35 | 890 | 0.97 | 0.04 | Klooster *et al.* (1999) |
| $NH_3$ | 165 | 22 | 362 | 0.45 | 0.06 | Boese *et al.* (1997) |
| $NH_2CN$ | 1542 | 407 | 2365 | 0.65 | 0.17 | Denner *et al.* (1988) |
| $OCl_2$ | 101 | 23 | 254 | 0.40 | 0.09 | Minkwitz *et al.* (1998) |
| $OC(NH_2)_2$ | 194 | 43 | 283 | 0.69 | 0.15 | Swaminathan *et al.* (1984) |

## 2. Methodology

### 2.1. Basic plan: comparison of structure factors calculated with and without correlation effects

To address the question of the experimental detectability of electron correlation effects in the X-ray structure factors, we must consider the difference between the measured X-ray structure factors and a set of hypothetical X-ray structure factors calculated without electron correlation – the so-called independent-particle or Hartree–Fock model. Correlation is usually defined as the difference between the exact value and the value obtained from the Hartree–Fock approximation. In a similar manner, we can assess the effects of chemical bonding on the structure factors by considering the difference between the measured X-ray structure factors and a set of hypothetical X-ray structure factors calculated from the promolecule or procrystal model.

Since we are only interested in estimates of the effect of electron correlation, we avoid the need for real experimental data by assuming that good quantum-chemical calculations are a reasonable model of reality. The assumption that the sum of the better quantum-chemical methods are a reasonable model of reality is well supported for calculations on small molecules in the gas phase, based on comparisons with geometrical parameters, vibrational frequencies and dissociation and rearrangement energies (Helgaker *et al.*, 2000).

### 2.2. Calculation method for the structure factors and selection of systems to be studied

Since X-ray diffraction necessarily involves data that are available from crystalline systems, it suggests that quantum-mechanical calculation techniques which are adapted to infinite crystal systems should be considered carefully. However, while calculations of structure factors for an entire crystalline system using *ab initio* methods are indeed possible (Saunders *et al.*, 1998) *via* a crystalline molecular orbital (CMO) approach, in these calculations the effects of electron correlation commonly included in molecular quantum-chemical calculations are not readily incorporated in a systematically improvable way. DFT methods can be used but they are not systematically improvable in the way traditional variational or perturbational calculations are improvable. Another problem with infinite crystal methods is that the basis sets of functions used in developing the solutions are typically quite small and cannot be readily increased in size for computational reasons (Pisani *et al.*, 1988).

Electron correlation effects can also be modelled by treating the crystal as an array of non-interacting molecules, *i.e.* the so-called independent-molecule (IM) method (Chandler *et al.*, 1994). Previous work has shown that experimental structure factors are adequately reproduced by the IM method as long as molecular wavefunctions were obtained using reasonable quantum-chemical methods with good basis sets, and as long as some model was used to account for thermal motion (Chandler *et al.*, 1994). Indeed, it was possible to decide, on the basis of the experimental data, which theoretical models were better or worse, and these results were in accord with expectations based on theoretical considerations.

In the IM approach, however, the effects of the crystal lattice cannot be easily accounted for, except by expanding the size of the molecular cluster representing the infinite crystal. For large clusters, this approach also becomes computationally impractical. In the present study, our intention is to see the effects of electron correlation and not the effects of chemical bonding between two different molecules. Therefore, in this paper, we have adopted the IM model to calculate small-molecule molecular crystal densities. Since all intermolecular effects are ignored in this approach, the dynamic correlation effects we are treating are necessarily intramolecular.

In experiments, the effects of the crystalline lattice would be minimized if attention was limited to molecular crystals composed of small molecules that interact solely through van der Waals forces, by virtue of the large relative separation of the molecules and the weakness of the interactions (Spackman *et al.*, 1999). In crystals where stronger interactions, such as hydrogen bonding, are present, the effects of the crystalline lattice on structure factors could be comparable with those from intramolecular correlation (Spackman *et al.*, 1999) and unravelling correlation from intermolecular effects could be difficult. Nevertheless, in this investigation equal numbers of non-hydrogen-bonded and hydrogen-bonded molecules were examined.

### 2.3. How to assess whether the effects are measurable

The central issue concerning the detectability of chemical bonding and correlation effects is to decide what constitutes an acceptable threshold for experimental detectability. Two methods have been used in this paper. The first is a naive *R*-factor-like criterion, while the second is a more sophisticated method based on real X-ray data for estimating experimental errors. We have used a measure related to the so-called '*R* factor', a statistic defined in equation (3) below, which is commonly used in the crystallographic community to measure agreement between data sets. Every crystal has its

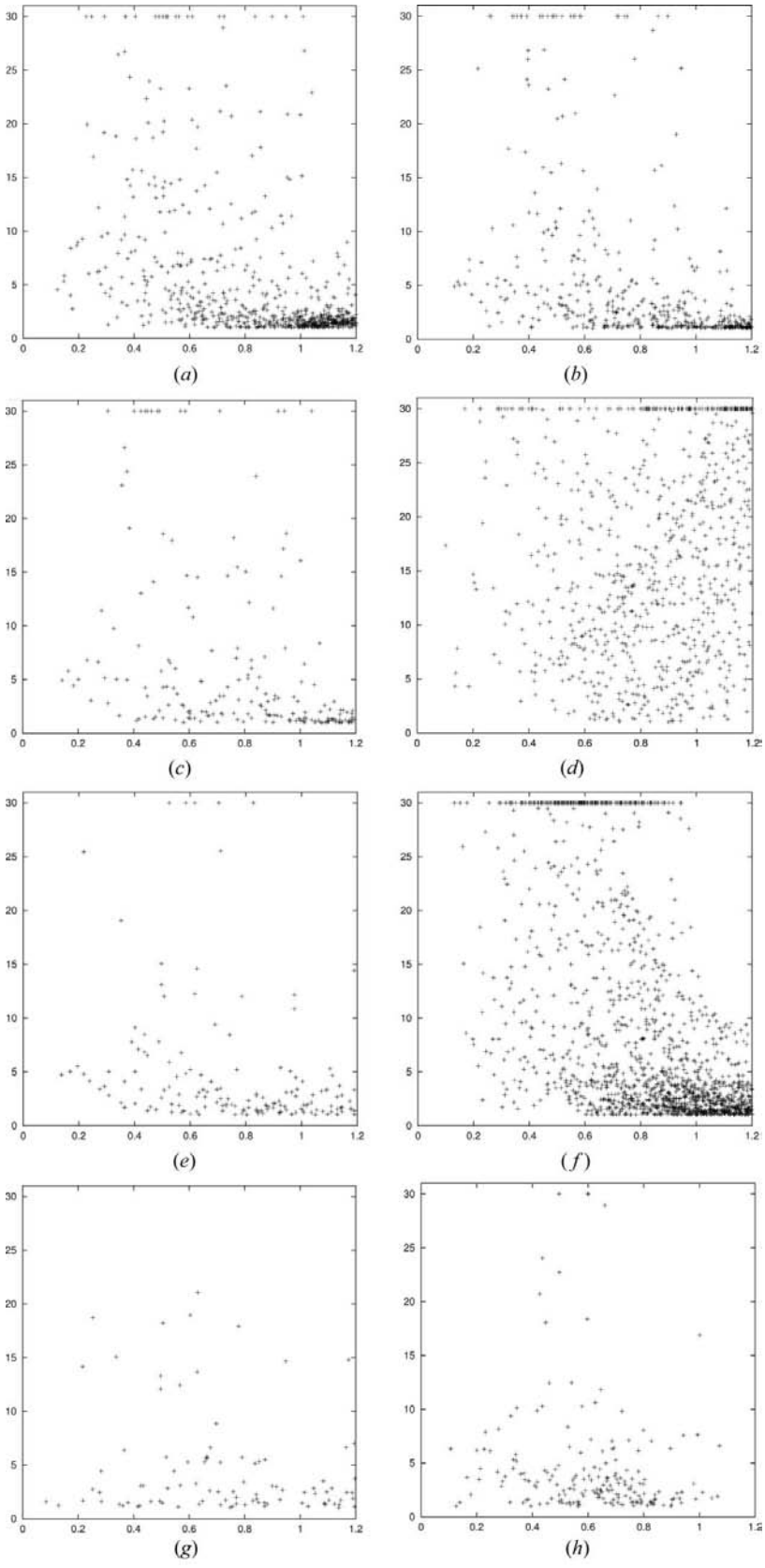


**Figure 1**
Plots of the % $R_{\mathrm{IAM:QCISD}}$ (vertical axis) against $\sin\theta/\lambda$ (Å$^{-1}$) (horizontal axis) for a series of molecular crystals, showing the effect of deviations from sphericity as a function of scattering angle. (*a*) $C_2H_6$, (*b*) $C_2H_4$, (*c*) $C_2H_2$, (*d*) $BH_3NH_3$, (*e*) $NH_3$, (*f*) $NH_2CN$, (*g*) $OCl_2$, (*h*) $OC(NH_2)_2$. Values greater than 30% have been set to 30% for display purposes.

own specific problems when it comes to collecting accurate and precise X-ray data, but the question is: what $R$ value might be achievable in favourable cases with present-day techniques?

In a recent study, Lippmann & Schneider (2000) used high-energy synchrotron radiation on cuprite and achieved an internal $R_{\mathrm{int}}(F^2)$ factor of 0.55%, with an internal consistency of at most 1.5% for individual reflections, collecting data up to $\sin\theta/\lambda < 1.5$ Å$^{-1}$, where $\theta$ is the X-ray scattering angle and $\lambda$ is the X-ray wavelength. Cuprite is a hard inorganic substance that has not presented other special problems. Nevertheless, urea, a much softer material with H atoms present, has been studied by Birkedal *et al.* (2004), who quoted a mean $|F^2|/\sigma_{F^2}$ of 49.9, implying a $\sigma_{F^2}/|F^2|$ value of 2% for their data. In the light of these recent data, we have adopted an optimistic threshold of 1% as an estimate of the change in the structure factors that might be detectable if careful experimental work is carried out using modern X-ray sources with particularly favourable crystals. We have used a conservative cut-off of $\sin\theta/\lambda < 1.2$ Å$^{-1}$. It may be possible to see relative changes smaller than 1% if one decides to focus attention and effort on just a few select reflections, as is done in experiments that try to detect the effects of the electric field on the structure factors (Hansen *et al.*, 2004), but we are concerned here with the generic X-ray diffraction experiment rather than such specialist experiments.

While the work cited on cuprite and urea represents some of the best available experiments, it is desirable to have an estimate of the errors in the structure-factor magnitudes that can be obtained in more typical experiments. We have therefore tried to estimate the $\sigma$'s directly, using as specific examples the data set for $NH_3$ (Boese *et al.*, 1997) and the one for $Na_3Co(NO_2)_6$ (Figgis & Sobolev, 2001) collected in our laboratories. We found that in each case the $\sigma$'s, where $I_{\mathrm{obs}} > 3\sigma(I_{\mathrm{obs}})$, could be fitted ($R < 0.2$) as a function of $I_{\mathrm{obs}}$:

$$\sigma(I_{\mathrm{obs},i}) = a + b(I_{\mathrm{obs},i})^c. \qquad (1)$$

For $NH_3$, the constants found in the above equations were $b = 0.0010$ and

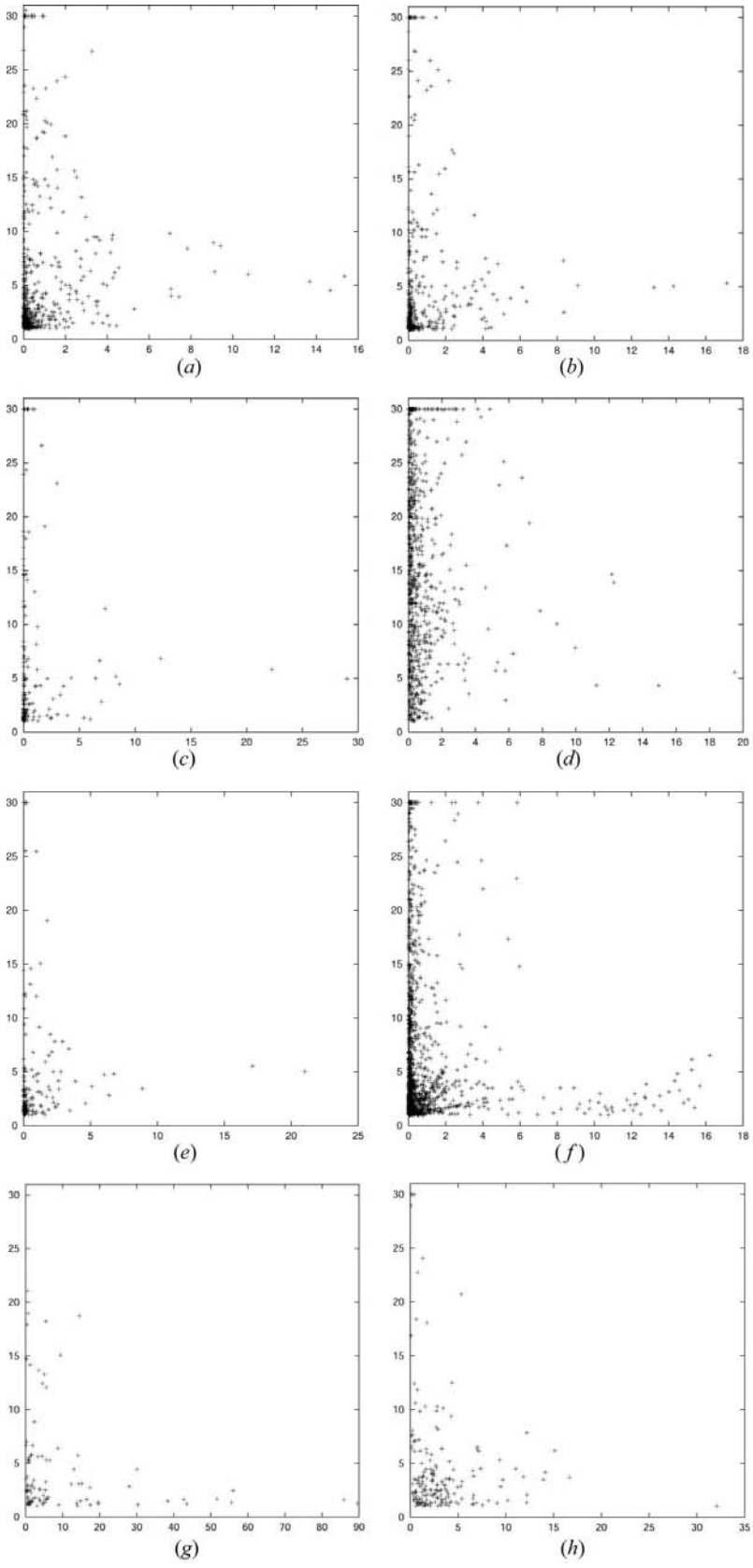


**Figure 2**
Plots of the % $R_{\mathrm{IAM:QCISD}}$ (vertical axis) against $|F_{\mathrm{QCISD}}|$ (horizontal axis), the magnitude of the QCISD structure factor, for a series of molecular crystals. (*a*) $C_2H_6$, (*b*) $C_2H_4$, (*c*) $C_2H_2$, (*d*) $BH_3NH_3$, (*e*) $NH_3$, (*f*) $NH_2CN$, (*g*) $OCl_2$, (*h*) $OC(NH_2)_2$. Values greater than 30% have been set to 30% for display purposes.

$c = 1.0$. For $Na_3Co(NO_2)_6$, the constants were $b = 0.0018$ and $c = 0.8$. We proceed, then, to construct the standard uncertainties for the $F^2$ data set for a molecule of interest by applying the constants $b$ and $c$ above to its reflections. For example, considering the case where $NH_3$ is the reference, the constant $a$ was then evaluated to give a minimum $\sigma$ with the same ratio to the maximum as is the case for $NH_3$. We then use the relationship

$$\sigma(|F_i|) = \sigma(F_i^2)/2|F_i|, \qquad (2)$$

where $|F_i|$ is the magnitude of the structure factor. We believe such sets of standard uncertainties allow a more realistic assessment of whether the differences between values of $F^2_{\mathrm{RHF}}$ and $F^2_{\mathrm{QCISD}}$ are experimentally significant. However, we reiterate that each crystal is different, and therefore the procedure used here to transfer $\sigma$'s from one crystal to another should be regarded with caution.

For individual symmetry-unique structure-factor magnitudes $|F_i(A)|$ and $|F_i(B)|$ calculated from two theoretical models, say $A$ and $B$, respectively, the percentage change between the two models is defined as

$$R_{A:B} = \frac{||F_i(A)| - |F_i(B)||}{|F_i(B)|} \times 100\%. \qquad (3)$$

Note that this expression is not symmetric in $A$ and $B$.

### 2.4. Calculation details

The wavefunction models for the IM calculations we have chosen to use in this study to calculate the electron density are:

(i) the independent-atom model (IAM) or promolecule density;

(ii) the Hartree–Fock (HF) model;

(iii) the quadratic configuration interaction model with single and double substitutions (QCISD);

(iv) the B3LYP density functional theory model.

The spherical-atom densities obtained for the promolecule density were calculated by spherically averaging the ground-state unrestricted-Hartree–Fock density for the isolated atoms.

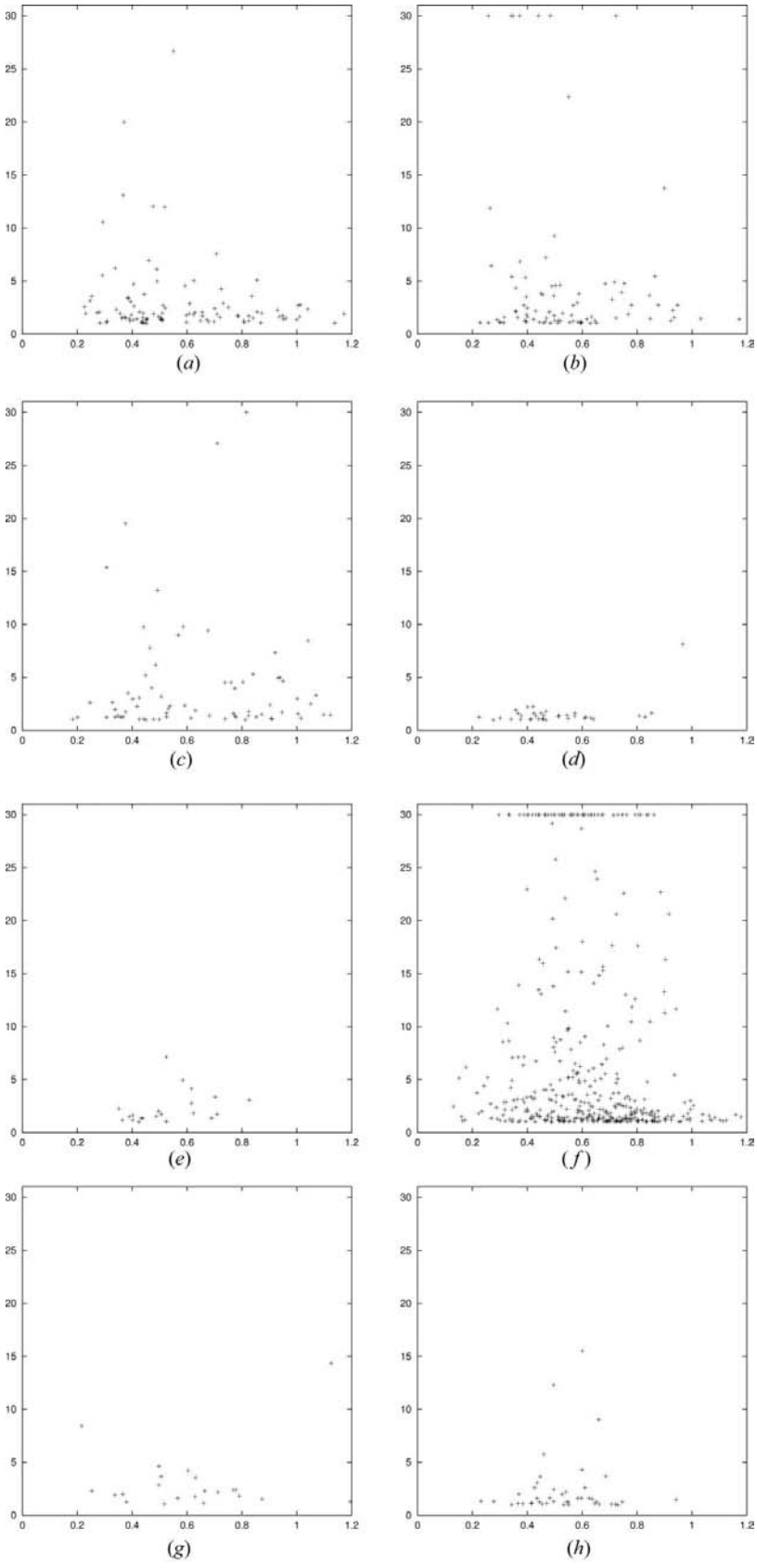


**Figure 3**
Plots of the % $R_{\mathrm{HF:QCISD}}$ (vertical axis) against $\sin\theta/\lambda$ (Å$^{-1}$) (horizontal axis) for a series of molecular crystals, showing the effect of electron correlation on simulated X-ray structure factors as a function of scattering angle. (*a*) $C_2H_6$, (*b*) $C_2H_4$, (*c*) $C_2H_2$, (*d*) $BH_3NH_3$, (*e*) $NH_3$, (*f*) $NH_2CN$, (*g*) $OCl_2$, (*h*) $OC(NH_2)_2$. Values greater than 30% have been set to 30% for display purposes.

A reasonably large cc-pVTZ basis set was used to include the effects of electron correlation as comprehensively as possible (Woon & Dunning, 1993). Such basis sets used in conjunction with the QCISD method have been shown in other studies to produce gas-phase geometries and frequencies extremely accurately (Hampel *et al.*, 1992). By necessity, only relatively small molecules, with light atoms, were included in this study. Only molecules with known crystal structures were chosen. The set of molecules examined in this work along with the references to the crystallographic geometrical parameters used in the calculations are given in Table 1.

Molecular charge-density distributions were calculated using the *Gaussian98* software package (Frisch *et al.*, 1998). The calculation of X-ray structure factors has been described before (Jayatilaka & Grimwood, 2001; Grimwood & Jayatilaka, 2001) and we use the *TONTO* program to evaluate these (Jayatilaka & Grimwood, 2000). In these structure-factor calculations, the effects of thermal motion were accounted for using Debye–Waller factors (*i.e.* Gaussian thermal ellipsoids) taken from experiment, the references for geometries and thermal parameters are given in Table 1 for each system studied. For all the calculations, the Stewart thermal averaging model was used (Stewart, 1969). The Tanaka model was used in two cases to check the effect of using different thermal averaging models (Tanaka, 1988). These models are discussed also in more detail in Jayatilaka & Grimwood (2001) and Grimwood & Jayatilaka (2001).

## 3. Results

### 3.1. The detectability of asphericity in X-ray structure-factor data

Table 1 shows the total number of structure factors with $\sin\theta/\lambda < 1.2$ Å$^{-1}$, where $\theta$ is the X-ray scattering angle and $\lambda$ is the X-ray wavelength, for a range of small-molecule molecular crystals. The table also shows the number of structure factors in this range which differ by more than 1% when comparing the spherical IAM model and the QCISD model and

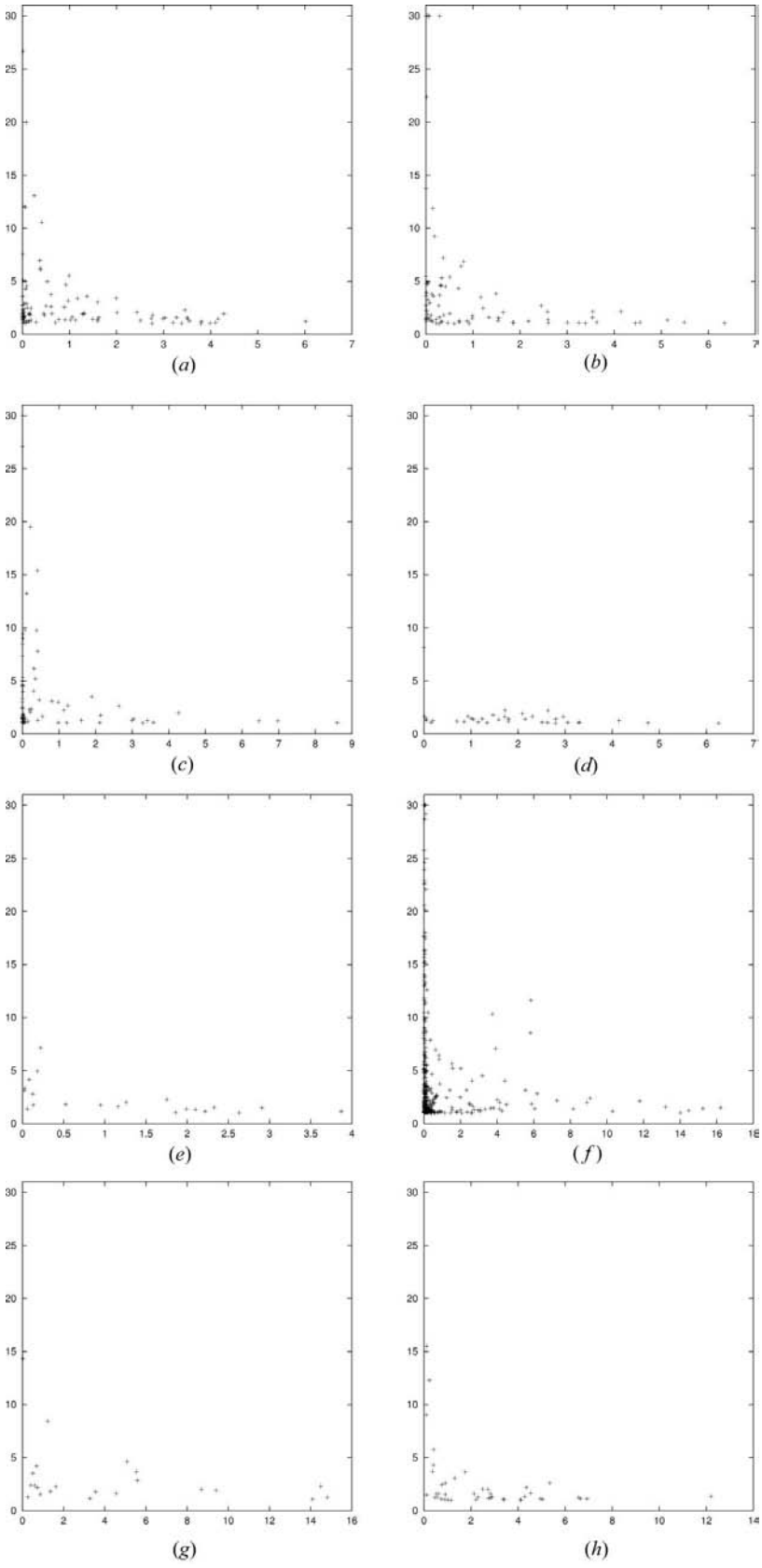


**Figure 4**
Plots of the % $R_{\rm HF:QCISD}$ (vertical axis) against $|F_{\rm QCISD}|$ (horizontal axis), the magnitude of the QCISD structure factor, for a series of molecular crystals. (*a*) $C_2H_6$, (*b*) $C_2H_4$, (*c*) $C_2H_2$, (*d*) $BH_3NH_3$, (*e*) $NH_3$, (*f*) $NH_2CN$, (*g*) $OCl_2$, (*h*) $OC(NH_2)_2$. Values greater than 30% have been set to 30% for display purposes.

when comparing the HF model and the QCISD model.

In almost all cases, at least 50% of the data, and in one case nearly 100% of the data show detectable deviations from sphericity. On the other hand, only about 10% of the data on average (and in one case only as little as 4% of the data) show correlation effects that might be detectable in very careful experiments. The raw number of data that shows these correlation effects obviously depends on a number of factors such as unit-cell size, and so on, but for this selection of small-molecule molecular crystals it is of the order of 100 reflections.

Fig. 1 shows the percentage changes in the structure factors on going from an independent-atom model to a QCISD model plotted against $\sin\theta/\lambda$. Although it is difficult to detect a consistent trend, most of the deviations seem to occur at higher angle, $\sin\theta/\lambda > 0.5$ Å$^{-1}$. It is acknowledged that the total number of reflections increases with $\sin\theta/\lambda$. However, the observation does mean that there tends to be more information in the data about changes in the density around the core than about the more interesting valence regions.

Fig. 2 shows the percentage changes in the structure factors of Fig. 1 plotted against the magnitude of the QCISD structure factor itself. It is clear that most of the reflections that change by more than 1% are in the lower intensity regime. It would appear that, while there is a large amount of data pertaining to the incorporation of atoms into a molecule, it may not always be easy to obtain all of the relevant information.

### 3.2. The detectability of electron correlation effects in X-ray structure-factor data

Fig. 3 shows the percentage changes between the HF and QCISD structure factors plotted against $\sin\theta/\lambda$. It is immediately apparent that many fewer significant data are contained in these plots, and most of the significant reflections lie toward the lower end of the range 0.2 to 0.8 Å$^{-1}$. It is also apparent that many of the reflections are only marginally above the 1% detectability threshold. Fig. 4 shows the same

**Table 2**
The differences between the structure factors $\Delta_{\mathrm{RHF-QCISD}} = F_{\mathrm{RHF}} - F_{\mathrm{QCISD}}$ and $\Delta_{\mathrm{RHF-B3LYP}} = F_{\mathrm{RHF}} - F_{\mathrm{B3LYP}}$ for $NH_2CN$.

The ratio of these differences to the estimated errors for each reflection is also given. The errors were estimated from the reference experimental data of $NH_3$ using the procedure described in the text.

| $h$ | $k$ | $l$ | $\sigma$ | $\Delta_{\mathrm{RHF-QCISD}}$ | $(\Delta_{\mathrm{RHF-QCISD}})/\sigma$ | $\Delta_{\mathrm{RHF-B3LYP}}$ | $(\Delta_{\mathrm{RHF-B3LYP}})/\sigma$ |
|---|---|---|---|---|---|---|---|
| 2 | 0 | 0 | 0.18 | 0.45 | 2.44 | 0.60 | 3.27 |
| 4 | 0 | 0 | 0.13 | −0.68 | −5.13 | −0.82 | −6.18 |
| 6 | 0 | 0 | 0.12 | −0.33 | −2.77 | −0.47 | −3.87 |
| 2 | 2 | 0 | 0.13 | 0.31 | 2.42 | 0.41 | 3.23 |
| 4 | 2 | 0 | 0.18 | −0.39 | −2.14 | −0.46 | −2.51 |
| 6 | 2 | 0 | 0.12 | −0.28 | −2.34 | −0.41 | −3.46 |
| 0 | 4 | 0 | 0.31 | −0.25 | −0.79 | −0.63 | −2.01 |
| 6 | 4 | 0 | 0.11 | −0.14 | −1.31 | −0.24 | −2.16 |
| 0 | 6 | 0 | 0.19 | −0.10 | −0.54 | −0.36 | −1.92 |
| 3 | 1 | 1 | 0.21 | 0.42 | 2.02 | 0.50 | 2.39 |
| 5 | 1 | 1 | 0.16 | −0.60 | −3.80 | −0.78 | −4.95 |
| 1 | 3 | 1 | 0.25 | −0.25 | −1.01 | −0.47 | −1.88 |
| 5 | 3 | 1 | 0.13 | −0.35 | −2.67 | −0.49 | −3.73 |
| 1 | 5 | 1 | 0.15 | −0.11 | −0.75 | −0.32 | −2.10 |
| 3 | 5 | 1 | 0.11 | −0.11 | −1.07 | −0.24 | −2.26 |
| 5 | 5 | 1 | 0.11 | −0.13 | −1.15 | −0.20 | −1.78 |
| 2 | 0 | 2 | 0.16 | 0.23 | 1.45 | 0.34 | 2.10 |
| 4 | 0 | 2 | 0.13 | −0.50 | −3.81 | −0.58 | −4.46 |
| 6 | 0 | 2 | 0.12 | −0.30 | −2.53 | −0.42 | −3.51 |
| 2 | 2 | 2 | 0.12 | 0.15 | 1.30 | 0.22 | 1.87 |
| 4 | 2 | 2 | 0.17 | −0.28 | −1.64 | −0.31 | −1.83 |
| 6 | 2 | 2 | 0.12 | −0.25 | −2.13 | −0.36 | −3.13 |
| 0 | 4 | 2 | 0.29 | −0.24 | −0.83 | −0.62 | −2.14 |
| 6 | 4 | 2 | 0.11 | −0.13 | −1.18 | −0.21 | −1.94 |
| 0 | 6 | 2 | 0.18 | −0.09 | −0.50 | −0.32 | −1.79 |
| 1 | 1 | 3 | 0.31 | −0.19 | −0.62 | −0.34 | −1.12 |
| 5 | 1 | 3 | 0.15 | −0.44 | −3.04 | −0.57 | −3.94 |
| 1 | 3 | 3 | 0.21 | −0.20 | −0.94 | −0.45 | −2.11 |
| 3 | 3 | 3 | 0.12 | −0.13 | −1.08 | −0.26 | −2.12 |
| 5 | 3 | 3 | 0.13 | −0.27 | −2.11 | −0.36 | −2.90 |
| 1 | 5 | 3 | 0.14 | −0.08 | −0.59 | −0.26 | −1.82 |
| 3 | 5 | 3 | 0.11 | −0.12 | −1.15 | −0.24 | −2.22 |
| 5 | 5 | 3 | 0.11 | −0.10 | −0.89 | −0.15 | −1.34 |
| 0 | 0 | 4 | 0.49 | −0.34 | −0.69 | −0.62 | −1.27 |
| 4 | 0 | 4 | 0.13 | −0.17 | −1.34 | −0.17 | −1.29 |
| 6 | 0 | 4 | 0.11 | −0.22 | −1.90 | −0.29 | −2.60 |
| 0 | 2 | 4 | 0.38 | −0.31 | −0.81 | −0.66 | −1.71 |
| 6 | 2 | 4 | 0.11 | −0.18 | −1.59 | −0.26 | −2.29 |
| 0 | 4 | 4 | 0.24 | −0.20 | −0.86 | −0.53 | −2.24 |
| 6 | 4 | 4 | 0.11 | −0.09 | −0.85 | −0.15 | −1.39 |
| 0 | 6 | 4 | 0.16 | −0.06 | −0.37 | −0.23 | −1.40 |
| 1 | 1 | 5 | 0.21 | −0.16 | −0.76 | −0.41 | −1.94 |
| 3 | 1 | 5 | 0.13 | −0.24 | −1.91 | −0.38 | −3.05 |
| 5 | 1 | 5 | 0.13 | −0.25 | −1.95 | −0.32 | −2.46 |
| 1 | 3 | 5 | 0.16 | −0.12 | −0.73 | −0.33 | −2.04 |
| 3 | 3 | 5 | 0.11 | −0.21 | −1.92 | −0.34 | −3.11 |
| 5 | 3 | 5 | 0.12 | −0.15 | −1.31 | −0.20 | −1.72 |
| 1 | 5 | 5 | 0.13 | −0.04 | −0.33 | −0.16 | −1.23 |
| 3 | 5 | 5 | 0.11 | −0.11 | −1.04 | −0.20 | −1.81 |
| 0 | 0 | 6 | 0.30 | −0.32 | −1.06 | −0.70 | −2.30 |
| 2 | 0 | 6 | 0.11 | −0.22 | −2.03 | −0.26 | −2.44 |
| 6 | 0 | 6 | 0.11 | −0.12 | −1.15 | −0.16 | −1.52 |
| 0 | 2 | 6 | 0.26 | −0.26 | −1.00 | −0.59 | −2.28 |
| 2 | 2 | 6 | 0.12 | −0.18 | −1.44 | −0.21 | −1.73 |
| 6 | 2 | 6 | 0.11 | −0.10 | −0.95 | −0.14 | −1.32 |
| 0 | 4 | 6 | 0.19 | −0.13 | −0.69 | −0.34 | −1.82 |
| 1 | 1 | 7 | 0.15 | −0.08 | −0.53 | −0.25 | −1.70 |
| 3 | 1 | 7 | 0.11 | −0.25 | −2.35 | −0.37 | −3.46 |
| 5 | 1 | 7 | 0.12 | −0.11 | −0.97 | −0.13 | −1.13 |
| 1 | 3 | 7 | 0.13 | −0.05 | −0.36 | −0.17 | −1.29 |
| 3 | 3 | 7 | 0.11 | −0.18 | −1.65 | −0.27 | −2.47 |
| 3 | 5 | 7 | 0.12 | −0.08 | −0.69 | −0.14 | −1.11 |
| 0 | 0 | 8 | 0.20 | −0.17 | −0.87 | −0.40 | −1.98 |
| 2 | 0 | 8 | 0.15 | −0.18 | −1.17 | −0.22 | −1.46 |
| 0 | 2 | 8 | 0.18 | −0.13 | −0.73 | −0.31 | −1.69 |
| 3 | 1 | 9 | 0.11 | −0.16 | −1.41 | −0.22 | −1.96 |
| 3 | 3 | 9 | 0.12 | −0.11 | −0.88 | −0.16 | −1.24 |

percentage differences but instead plotted against the magnitude of the structure factor. Although most of the reflections lie toward the lower end of the intensity scale, there are some reflections toward the higher end, and there are fewer as the intensity increases. Applying an overall 1% detectability threshold is misleading in the situation revealed in Fig. 4. The errors obtained in X-ray diffraction experiments are a much larger fraction of the magnitude of the measured structure factors for low-intensity reflections. Consequently, whereas a 1% change in a structure factor may be readily observed for high- and moderate-intensity reflections, the standard uncertainties for low-intensity reflections may make detection of this change impossible. Since so many of the large changes in structure factors caused by correlation are at low $|F_{\mathrm{QCISD}}|$ values, it was judged to be important to compare the changes in structure factors with some experimentally realistic $\sigma$ values being assigned to each reflection. $NH_2CN$ was selected for a closer examination because, as is evident from Fig. 3, it shows the greatest number of % $R_{\mathrm{HF:QCISD}}$ larger than 1%. Using the procedure detailed in the methodology section, $\sigma$'s were associated with each theoretical reflection by reference to data for $NH_3$ and $Na_3Co(NO_2)_6$. The likelihood of any one reflection being suitable for detecting the effects of correlation was determined by taking the differences $\Delta_{\mathrm{RHF-QCISD}} = F_{\mathrm{RHF}} - F_{\mathrm{QCISD}}$ and $\Delta_{\mathrm{RHF-B3LYP}} = F_{\mathrm{RHF}} - F_{\mathrm{B3LYP}}$, and forming the ratio $\Delta/\sigma$ for the respective structure factors. The results for $NH_2CN$ where the $\sigma$'s were estimated from data for $NH_3$ are collected in Table 2. The results for $\sigma$'s estimated from $Na_3Co(NO_2)_6$ are similar. Only the ratios, $\Delta/\sigma$, that were greater than 1, for either $\Delta_{\mathrm{RHF-QCISD}}$ or $\Delta_{\mathrm{RHF-B3LYP}}$, are recorded. The table includes information that is additional to that appearing in the figures as it contains data relating to the B3LYP calculations as well as that from the QCISD wavefunction.

From Table 2, it is clear, as would be expected, that the densities from QCISD and B3LYP calculations are very similar. In all but one reflection, 404, $|\Delta/\sigma|$ is larger for the B3LYP results. This is reflected in the fact that 26 of the differences, $\Delta_{\mathrm{RHF-QCISD}}$, are less than the respective $\sigma$ whereas none of the B3LYP structure factors are like this. We may judge that it is necessary for structure factors to differ from each other by more than $3\sigma$ for a measurement to have statistical significance. The differences recorded in the table indicate measurements on most reflections would not produce statistically significant data. For the $\Delta_{\mathrm{RHF-QCISD}}$, there are only four reflections with ratios greater than $3\sigma$. It is better for the B3LYP example where there are 14 reflections greater than $3\sigma$. However, there are so few data differing significantly from experimental error bounds that it would appear unlikely that correlation effects could be discerned experimentally in a conventional X-ray experiment.

### 3.3. Testing the assumption that QCISD forms a good model of the electron density

The validity of our assumption that the QCISD model is a good model of reality has been tested to some extent by replacing the QCISD calculations with B3LYP calculations. The B3LYP model is known also to produce highly accurate results for small-molecule systems. Fig. 5 is a plot of the percentage change between the HF and B3LYP structure factors *versus* $|F_{\rm B3LYP}|$ for two example cases, $C_2H_2$ and $BH_3NH_3$. The plots show that the distribution of the detectable data is very similar to that seen in Figs. 4(*c*) and 4(*d*), respectively. We have also directly compared the structure factors obtained from QCISD and B3LYP calculations for $C_2H_2$ and $BH_3NH_3$ in Fig. 6. The percentage differences in the structure factors are approximately 2% for those reflections that have a significant magnitude.

### 3.4. Testing the assumption that the Stewart thermal averaging model is adequate

The structure factors described above were all calculated using the Stewart thermal averaging model to account for the effects of thermal motion. It is therefore of interest to see if the results obtained are sensitive to the use of another model. Fig. 7 is a plot of the percentage changes in the structure factors when the Tanaka thermal averaging model was used, when comparing IAM and QCISD results for $C_2H_2$ and $BH_3NH_3$. Comparing this figure with Figs. 2(*c*) and 2(*d*) shows hardly any change in the overall distribution of points. Thus, the use of a different thermal averaging model does not significantly affect the amount of data available for detecting the effects of non-sphericity. Likewise, Fig. 8 shows the percentage change in individual structure factors when comparing HF and QCISD calculations which use the Tanaka thermal averaging model, again for $C_2H_2$ and $BH_3NH_3$; and again, the distribution is similar to those in plots (*c*) and (*d*) of Fig. 4, which were calculated using the Stewart thermal averaging model.

We have also made plots (not shown) comparing the structure factors from the Tanaka method and the Stewart method. These plots show that, for the reflections which have a significant magnitude, most of the structure-factor predictions are within 2.5% of each other. For the weak reflections, the percentage changes are of course much larger since a small absolute change results in a large percentage change.

## 4. Conclusions

Deviations from atom sphericity in the structure factors are clearly distinguishable in the structure factors. At least half of the data shows changes greater than 1%, and changes of the

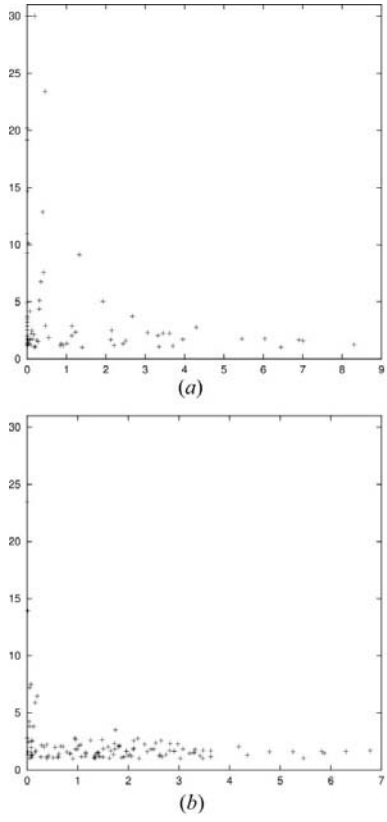


**Figure 5**
Plots of the % $R_{\rm HF:B3LYP}$ (vertical axis) against $|F_{\rm B3LYP}|$ (horizontal axis), the magnitude of the B3LYP structure factor, for two representative molecular crystals. (*a*) $C_2H_2$, (*b*) $BH_3NH_3$. Values greater than 30% have been set to 30% for display purposes.

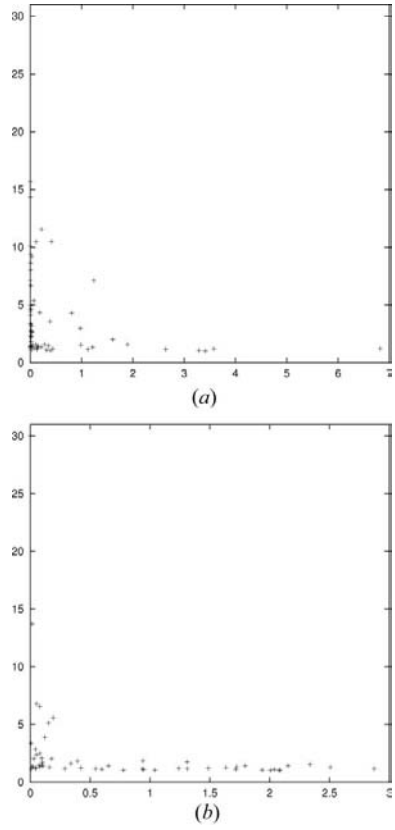


**Figure 6**
Plots of the % $R_{\rm B3LYP:QCISD}$ (vertical axis) against $|F_{\rm QCISD}|$ (horizontal axis), the magnitude of the QCISD structure factor, for two representative molecular crystals. (*a*) $C_2H_2$, (*b*) $BH_3NH_3$.

order of 20% are often observed. It should be noted, however, that many of these reflections are not very intense, the corresponding structure factors often being below 0.5 e per asymmetric unit. Since these calculations are so easy to perform, it would be worthwhile performing them before attempting a detailed high-accuracy high-precision X-ray study in order to establish those reflections that should be paid greater care and attention, from an experimental point of view. In particular, such calculations should give an idea of whether the ratio of model parameters to the *significant* portion of the experimental data is adequate or not.

The effects on the structure factors due to intramolecular electron correlation are much smaller than the effects of asphericity – often only just above the 1% detectability threshold used in this paper – and so are about one to two orders of magnitude smaller than deviations from sphericity. Furthermore, only 10% of the total data with $\sin\theta/\lambda < 1.2$ Å$^{-1}$ are significant for detecting these correlation effects; of those 10%, many are at low intensity. The significance of this result is that very careful experiments will be necessary to produce data that are useful for quantitative modelling of electron correlation effects. Whether such experiments are currently feasible was tested by comparison of the theoretically predicted changes with standard errors estimated from typical experiments.

The conclusion is that it is unlikely that X-ray experiments performed under current limitations would be capable of detecting correlation effects in small molecules. The corollary to this is that it throws doubt on the explanation that intramolecular electron correlation is an important factor in disagreements that have been observed between experimentally and theoretically derived electron-difference-density maps. It is granted that the molecules used in the present study are small in comparison with the size of molecules usually studied experimentally, indicating that we should make a similar study on larger molecules. In addition, there are whole classes of molecules where there are near degeneracies (*e.g.* transition-metal compounds). These will display non-dynamic correlation effects which may lead to much larger changes in the structure factors.

Structure factors obtained from QCISD and B3LYP calculations were compared and the B3LYP calculations produce changes in the X-ray structure factors which are very similar to the QCISD results. Thus our conclusions about the amount of significant data relating to correlation effects is independent of whether QCISD or B3LYP is used for the electron correlation model. However, percentage differences in the structure factors amount to approximately 2% for the larger reflections. This suggests an experimental approach which concentrates on only a few reflections, for which it is known beforehand that correlation has a larger effect.

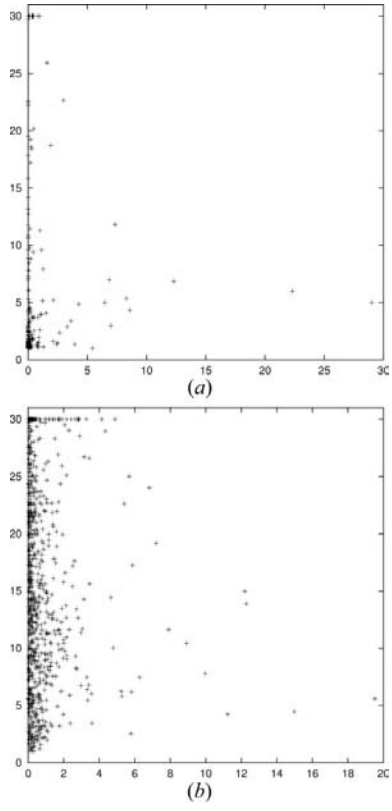


**Figure 7**
Plots of the % $R_{\mathrm{IAM:QCISD}}$ calculated using the Tanaka thermal averaging model (vertical axis) against $|F_{\mathrm{QCISD}}|$ (horizontal axis), the magnitude of the QCISD structure factor, for two representative molecular crystals. (*a*) $C_2H_2$, (*b*) $BH_3NH_3$. Values greater than 30% have been set to 30% for display purposes.

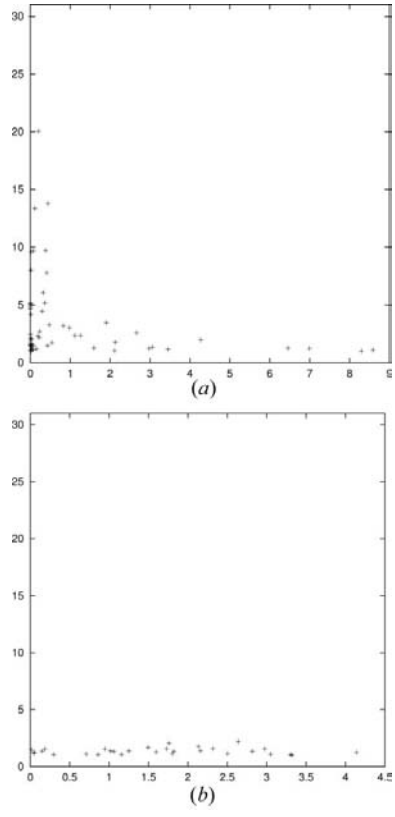


**Figure 8**
Plots of the % $R_{\mathrm{HF:QCISD}}$ calculated using the Tanaka thermal averaging model (vertical axis) against $|F_{\mathrm{QCISD}}|$ (horizontal axis), the magnitude of the QCISD structure factor, for two representative molecular crystals. (*a*) $C_2H_2$, (*b*) $BH_3NH_3$.

Although thermal averaging effects affect the magnitude of the structure factors (by about 2.5%), the overall conclusions about the detectability of the correlation effects are not changed by the use of different models for thermal averaging. It should be noted that different thermal averaging models produce changes in the structure factors of the same order as correlation effects, and the effects of different models for the correlation effects, and so correlation effects on the electron density will be difficult to deconvolute from thermal motion effects.

IB and DJ acknowledge helpful discussions with Professor David Rae. DJ acknowledges funding from the Australian Research Council Senior Fellowship scheme, and DJ and GSC acknowledge funding from the Discovery Grants scheme. DJ also acknowledges the Research School of Chemistry at the Australian National University for a visiting fellowship.

## References

Bader, R. F. W. & Chandra, A. K. (1968). *Can. J. Chem.* **46**, 953–966.
Becker, P. J., Gillet, J. M., Cortona, P. & Ragot, S. (2001). *Theor. Chem. Acc.* **105**, 284–291.
Bentley, J. J. & Stewart, R. F. (1976). *Acta Cryst.* A**32**, 910–914.
Birkedal, H., Madsen, D., Mathiesen, R. H., Knudsen, K., Weber, H. P., Pattison, P. & Schwarzenbach, D. (2004). *Acta Cryst.* A**60**, 371–381.
Boese, R., Niederprüm, N., Bläser, D., Maulitz, A., Antipin, M. & Mallinson, P. R. (1997). *J. Phys. Chem.* B**101**, 5794–5799.
Boyd, R., Wang, J. & Eriksson, L. (1995). *Recent Advances in Density Functional Methods*, p. 369. Singapore: World Scientific.
Boyd, R. J. & Wang, L. C. (1989). *J. Comput. Chem.* **10**, 367–375.
Chandler, G. S., Figgis, B. N., Reynolds, P. A. & Wolff, S. K. (1994). *Chem. Phys. Lett.* **225**, 421–426.
Chong, D. (1995). *Recent Advances in Density Functional Methods (Part I)*. Singapore: World Scientific.
Chong, D. (1997). *Recent Advances in Density Functional Methods (Part II)*. Singapore: World Scientific.
Coppens, P. (1997). *X-ray Charge Densities and Chemical Bonding*. New York: Oxford University Press.
Coppens, P. & Hall, M. B. (1982). *Electron Distributions and the Chemical Bond*. New York: Plenum.
Dawson, B. (1967). *Proc. R. Soc. London Ser. A*, **298**, 255–263.
Denner, L., Luger, P. & Buschmann, J. (1988). *Acta Cryst.* C**44**, 1979–1981.
Epstein, J., Bentley, J. J. & Stewart, R. F. (1977). *J. Chem. Phys.* **66**, 5564–5567.
Figgis, B. N. & Sobolev, A. N. (2001). *Acta Cryst.* C**57**, 885–886.
Frisch, M. J., Trucks, G. W., Schlegel, H. B., Scuseria, G. E., Robb, M. A., Cheeseman, J. R., Zakrzewski, V. G., Montgomery, J. A. Jr, Stratmann, R. E., Burant, J. C., Dapprich, S., Millam, J. M., Daniels, A. D., Kudin, K. N., Strain, M. C. *et al.* (1998). *Gaussian 98, Revision A.7*. Gaussian, Inc., Pittsburgh, PA, USA.
Gatti, C., McDougall, P. J. & Bader, R. F. W. (1988). *J. Chem. Phys.* **88**, 3792.
Grimwood, D. J. & Jayatilaka, D. (2001). *Acta Cryst.* A**57**, 87–100.
Hampel, C., Peterson, K. A. & Werner, H.-J. (1992). *Chem. Phys. Lett.* **190**, 1–12.
Hansen, N. K., Fertey, P. & Guillot, R. (2004). *Acta Cryst.* A**60**, 465–471.
Helgaker, T., Jørgensen, P. & Olsen, J. (2000). *Molecular Electronic Structure Theory*. New York: Wiley.
Hollister, C. & Sinanoğlu, O. (1966). *J. Am. Chem. Soc.* **88**, 13–21.
Howard, S. T., Hursthouse, M. B., Lehmann, C. W., Mallinson, P. R. & Frampton, C. S. (1992). *J. Chem. Phys.* **97**, 5616–5630.
Jayatilaka, D. & Grimwood, D. J. (2000). *Tonto: a Research Tool for Quantum Chemistry*. The University of Western Australia, Nedlands, Western Australia, Australia.
Jayatilaka, D. & Grimwood, D. J. (2001). *Acta Cryst.* A**57**, 76–86.
Klooster, W. T., Koetzle, T. F., Siegbahn, P. E. M., Richardson, T. B. & Crabtree, R. H. (1999). *J. Am. Chem. Soc.* **121**, 6337–6343.
Lippmann, T. & Schneider, J. R. (2000). *J. Appl. Cryst.* **33**, 156–167.
McMullan, R. K., Kvick, A. & Popelier, P. (1992). *Acta Cryst.* B**48**, 726–731.
Minkwitz, R., Bröchler, R. & Borrmann, H. (1998). *Z. Kristallogr.* **213**, 237.
Moszynski, R. & Szalewicz, K. (1987). *J. Phys. B*, **20**, 4347.
Nes, G. J. H. van & Vos, A. (1978). *Acta Cryst.* B**34**, 1947–1956.
Nes, G. J. H. van & Vos, A. (1979). *Acta Cryst.* B**35**, 2593–2601.
Ortiz-Henarejos, E. & San-Fabian, E. (1997). *Int. J. Quantum Chem.* **61**, 245–252.
Pisani, C., Dovesi, R. & Roetti, C. (1988). *Hartree–Fock Ab-Initio Treatment of Crystalline Systems, Lecture Notes in Chemistry*, Vol. 48. Heidelberg: Springer Verlag.
Reeuwijk, S. J. van, van Beek, K. G. & Feil, D. (2000). *J. Phys. Chem.* A**104**, 10901–10912.
Ritchie, J. P., King, H. F. & Young, W. S. (1986). *J. Chem. Phys.* **85**, 5175–5182.
Saunders, V. R., Dovesi, R., Roetti, C., Causà, M., Harrison, N. M., Orlando, R. & Zicovich-Wilson, C. M. (1998). *CRYSTAL 98 Users Manual*. University of Torino, Torino, Italy.
Silverstone, H. J. & Sinanoğlu, O. (1966). *J. Chem. Phys.* **44**, 1899–1907.
Sinanoğlu, O. (1961). *Proc. Natl Acad. Sci. USA*, **47**, 1217–1226.
Smith, V. H. (1977). *Phys. Scr.* **15**, 147–162.
Spackman, M. A., Byrom, P. G., Alfredsson, M. & Hermansson, K. (1999). *Acta Cryst.* A**55**, 30–47.
Stephens, M. E. & Becker, P. J. (1983). *Mol. Phys.* **49**, 65–89.
Stewart, R. F. (1969). *J. Chem. Phys.* **51**, 4569–4577.
Stewart, R. F. (1976). *Acta Cryst.* A**32**, 565–574.
Streltsov, V. A., Nakashima, P. N. H. & Johnson, A. W. S. (2003). *Microsc. Microanal.* **9**, 419–427.
Swaminathan, S., Craven, B. M. & McMullan, R. K. (1984). *Acta Cryst.* B**40**, 300–306.
Tanaka, K. (1988). *Acta Cryst.* A**44**, 1002–1008.
Wang, J., Eriksson, L. A., Boyd, R. J., Shi, Z. & Johnson, B. G. (1994). *J. Phys. Chem.* **98**, 1844–1850.
Wang, J., Eriksson, L. A., Johnson, B. G. & Boyd, R. J. (1996). *J. Phys. Chem.* **100**, 5274–5280.
Wang, J., Johnson, B. G., Boyd, R. J. & Eriksson, L. A. (1996). *J. Phys. Chem.* **100**, 6317–6324.
Wang, J., Shi, Z., Boyd, R. J. & Gonzalez, C. A. (1994). *J. Phys. Chem.* **98**, 6988–6994.
Woon, D. E. & Dunning, T. H. (1993). *J. Chem. Phys.* **98**, 1358–1371.
Zavodnik, V., Stash, A., Tsirelson, V., de Vries, R. & Feil, D. (1999). *Acta Cryst.* B**55**, 45–54.